

Article

Endoplasmic Reticulum-Targeting Two-Photon Fluorescent Probe for CYP1A Activity and Its Imaging Application in Endoplasmic Reticulum Stress

Chao Shi ^{1,2,†}, Yan Wang ^{2,†}, Xiangge Tian ¹, Xia Lv ², Yue An ¹, Jing Ning ^{1,2,*}, Xiulan Xin ³, Li Dai ^{1,*}, Xiaochi Ma ¹  and Lei Feng ^{1,4,5,*}

¹ Second Affiliated Hospital, Dalian Medical University, Dalian 116023, China

² College of Pharmacy, Dalian Medical University, Dalian 116044, China

³ College of Bioengineering, Beijing Polytechnic, Beijing 100029, China

⁴ School of Chemistry and Chemical Engineering, Henan Normal University, Xinxiang 453007, China

⁵ Key Laboratory of Emergency and Trauma of Ministry of Education, Hainan Medical University, Haikou 571199, China

* Correspondence: ningjing0626@163.com (J.N.); daily21st@aliyun.com (L.D.); leifeng@dmu.edu.cn (L.F.)

† These authors contributed equally to this work.

Abstract: Cytochrome P450 1A is one of the vital subfamilies of heme-containing cytochrome P450 enzymes belonging to an important exogenous metabolizing CYP in human. The abnormal of endoplasmic reticulum (ER) may directly affect the functional activity of ER-located CYP1A and be associated with the occurrence and development of various diseases. In the present study, we constructed a selective two-photon fluorescent probe **ERNM** for rapid and visual detection of endogenous CYP1A that was localized in the ER. **ERNM** could target the ER and detect the enzymatically active CYP1A in living cells and tissues. The monitoring ability of **ERNM** for the fluctuations in functionality level of CYP1A was confirmed using ER stressed A549 cell. Based on the ER-targeting two-photon probe for CYP1A, the close association of ER state and the functional activity of ER-locating CYP1A was confirmed, which would promote the deep understanding of the biofunction of CYP1A in various ER-related diseases.

Keywords: cytochrome P450 1A; fluorescent probe; endoplasmic reticulum-targeting; enzymatically active probe; two-photon



Citation: Shi, C.; Wang, Y.; Tian, X.; Lv, X.; An, Y.; Ning, J.; Xin, X.; Dai, L.; Ma, X.; Feng, L. Endoplasmic Reticulum-Targeting Two-Photon Fluorescent Probe for CYP1A Activity and Its Imaging Application in Endoplasmic Reticulum Stress.

Molecules **2023**, *28*, 3472. <https://doi.org/10.3390/molecules28083472>

Academic Editors: Haiying Liu, Wei Gong, Yao Sun, Haidong Li and Van-Nghia Nguyen

Received: 16 February 2023

Revised: 10 April 2023

Accepted: 10 April 2023

Published: 14 April 2023



Copyright: © 2023 by the authors. Licensee MDPI, Basel, Switzerland. This article is an open access article distributed under the terms and conditions of the Creative Commons Attribution (CC BY) license (<https://creativecommons.org/licenses/by/4.0/>).

1. Introduction

Cytochrome P450 (CYP) is a large family of hemoproteins, which mediates various oxidative transformations in nature [1,2]. CYP1A is one of the subfamilies which consists of the structurally and functionally related isoforms CYP1A1 and CYP1A2, belonging to the important exogenous metabolizing CYP in human [3–5]. Imipramine, theophylline, caffeine and propranolol, and environmental toxicants including polycyclic aromatic hydrocarbons (PAH) and heterocyclic aromatic amines/amides (HAA) are all small-molecule ligands of CYP1A. Aside from mediating the metabolism of many commonly used clinical drugs, CYP1A also plays an important role in the bioactivation of pro-carcinogens PAH and HAA to the carcinogenic reactive intermediates which can bind to DNA or proteins, thereby contributing to the tumorigenesis and development of cancer and implications in some toxicity events [3]. Notably, except for the key role in oxidative metabolism of exogenous substance, the accumulating evidence supporting that CYP1A is involved in various significant biological processes, for example, the balance of oxidative state and oxidative stress, thereby were associated with a variety of diseases including liver injury, renal hypertension, hypertoxic lung injury, reproductive toxicity, etc. [6,7]. Therefore, the expression and functional activity of CYP1A in different tissues and specific or-

ganelles in cells may have some important implications for prevention and treatment of the involved diseases.

Endoplasmic reticulum (ER) is the largest organelle in cells made of a single membrane, which plays a significant role in different biosystems and mediates the various essential biological processes in cells, such as synthesis of extracellular lipoprotein, modification of proteins, and regulation of intracellular free calcium concentration [8,9]. Therefore, the change in physiological status for ER and the balance of some substances in ER are important affecting factors of the pathogenesis of many diseases [8,9]. The abnormal of endoplasmic reticulum and imbalance of the key substance may directly affect the functional activity of ER-located CYP1A and be associated with the occurrence and development of diseases [10,11]. Therefore, some relevant tool molecules are needed to study the changes in CYP1A activity in the endoplasmic reticulum under different physiological and pathological conditions, and to deeply uncover the relationship between the CYP1A activity and ER state, as well as the CYP1A activity and pathogenesis of diseases.

Fluorescence imaging technique displays many advantages that are not limited exclusively to its outstanding sensitivity, fast response, and superior spatiotemporal resolution. For this reason, this technique is nowadays widely used in environmental monitoring, drug screening, and physiological and pathological process evaluation, as well as other major areas [12–17]. Particularly, the two-photon fluorescence imaging possesses the higher resolution, deep penetration, low background, etc. that has received wide attention in recent years [18–21]. Considering the important biological functions of CYP1A, several reactive small molecule fluorescent probes that target CYP1A have been developed [22–24]. The CYP1A activity could be used to realize the real-time monitoring of CYP1A activity in cells and tissues, making it more accessible and facilitating further investigations of CYP1A-associated physiological and pathological processes. However, the ER-targeted two-photon fluorescent probes that could detect CYP1A activity are still lacking. Therefore, the two-photon molecular tool that can realize ER-targeted CYP1A activity imaging deserves to be explored for understanding the interaction effect between CYP1A and ER.

In the present study, we developed a two-photon fluorescent probe that could realize the activity detection of ER-located CYP1A. The fluorescent probe **ERNM** preferentially locates in ER of the cells, which attributes to the introduction of *p*-methylbenzene sulfonamide group to the distal end of the metabolic recognition site on the fluorophore naphthalimide. It was successfully used in detecting CYP1A in living cells and tissues by two-photon fluorescence imaging, thereby facilitating the location detection of CYP1A activity in complex biological systems. Using this fluorescent molecular tool **ERNM**, the activity changes in CYP1A under ER stress were effectively detected, which indicated the practical applications in uncovering the important roles of CYP1A in ER-related diseases.

2. Results and Discussion

2.1. Design and Synthesis of **ERNM**

Naphthalimide, as a classical fluorophore, has high fluorescence quantum yield, and the imide bond has strong electron absorption ability. Its fluorescence spectrum can be adjusted by changing the substituent group at C4 or C5, and its structural modification is relatively simple. In addition, naphthalimide has a two-photon fluorescence property, which gives it a unique advantage in biological applications. Here, *p*-methylbenzene sulfonamide group is first introduced into naphthalimide fluorophore, which has an endoplasmic reticulum targeting function, and methoxy is then introduced at the C4 site as the recognition site of CYP1A. **ERNM** was synthesized from 4-bromo-1,8-naphthalic anhydride in a two-part reaction. After the metabolism of **ERNM** through CYP1A, the methoxyl group became an oxygen anion, and the electron donor ability became stronger, resulting in significant changes in fluorescence intensity; therefore, **ERNM** could be used as a fluorescent probe for the detection of CYP1A.

2.2. Spectroscopic Response of ERNM toward CYP1A

In the first instance, the spectral properties of the designed probe ERNM toward CYP1A were investigated. The addition of increasing concentrations of CYP1A1 and CYP1A2 led the fluorescence intensity to gradually increase (Figure 1A,C). Furthermore, the fluorescence intensity at 558 nm increased linearly by adding increasing concentrations of CYP1A1 and CYP1A2 (0 to 20 nM), and the linear equations are $Y = 1371X + 523.2$ ($R^2 = 0.997$) for CYP1A1 and $Y = 1538X + 252.1$ ($R^2 = 0.991$) for CYP1A2, respectively (Y means fluorescence intensity and X means enzyme concentrations of CYP1A1 and CYP1A2). Additionally, the fluorescence intensity at 558 nm gradually increased from 0 to 30 min when ERNM was incubated with CYP1A1 and CYP1A2, respectively (Supplementary Figure S1). The distinct fluorescence response indicated that CYP1A-mediated demethylation of ERNM liberates the oxygen atom as a strong electron donor in the D- π -A structure, confirming the presence of intramolecular charge transfer (ICT) effects (Scheme 1). Additionally, the demethylated product of ERNM exhibited a high fluorescence output signal over the pH range of 4–12, while ERNM consistently exhibited extremely weak fluorescence. These results indicated that ERNM could be used as a molecular tool to detect the activity of CYP1A in physiological process (Supplementary Figure S2).

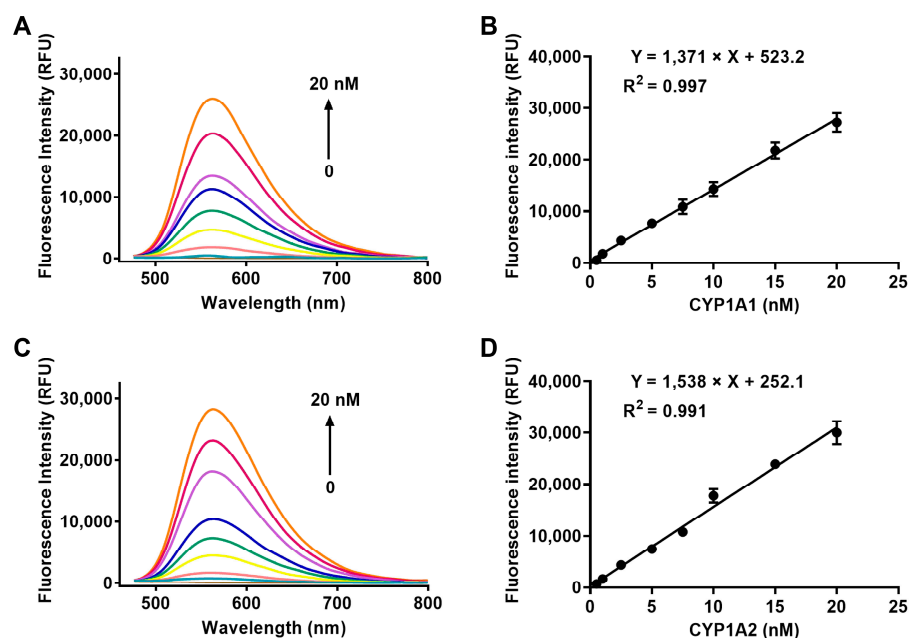
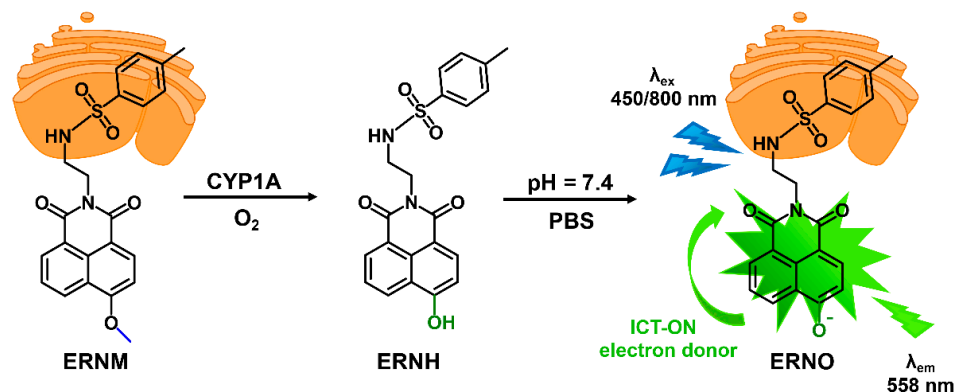


Figure 1. Fluorescence spectra of ERNM that incubated with increasing concentrations of CYP1A1 (A) and CYP1A2 (C). Fluorescence intensity of ERNM at 558 nm that incubated with various concentrations of CYP1A1 and CYP1A2. $\lambda_{\text{ex}} = 450$ nm. Data in (B,D) are shown as the mean \pm SD.



Scheme 1. Proposed mechanism of CYP1A triggering the fluorescence response of ERNM.

2.3. Selectivity Analysis of ERNM

The selectivity of **ERNM** for various CYP isoenzymes and potential interfering substances was further confirmed. The recombinant human CYP in vitro incubation assay indicated that CYP1A1/1A2 mediated the generation of fluorescence signals at 558 nm over other CYP isoenzymes including CYP1B1, CYP2A6, CYP2A13, CYP2B6, CYP2C8, CYP2C9, CYP2C18, CYP2C19, CYP2D6, CYP2E1, CYP2J2, CYP3A4, CYP3A5, CYP4A11, CYP4F2, CYP4F3, and CYP4F12 (Figure 2). Furthermore, the specificity of **ERNM** in complex biological samples was confirmed using subtype-selective inhibitors of CYP isoenzymes. The generation of the fluorescence signal can be sufficiently suppressed by CYP1A selective inhibitor (α -naphthoflavone), in comparison with the control group and another inhibitory group using TEPA (N,N',N''-triethylene thiophosphoramidate), montelukast, sulfaphenazolum, omeprazole, quinidine, chlormethiazole, and ketoconazole (Supplementary Figure S3). Additionally, the fluorescence response of **ERNM** was hardly affected during incubation with various potential interfering species, including common ion (Mn^{2+} , Ca^{2+} , Mg^{2+} , Ni^{2+} , Zn^{2+} , Sn^{4+} , K^+ , Fe^{3+} , Na^+ , Ba^{2+}) and amino acid (Ser, Trp, Gly, Arg, Cys, GSH) (Supplementary Figure S4). The relative results indicated the high specificity of **ERNM** for CYP1A in complex bio-samples.

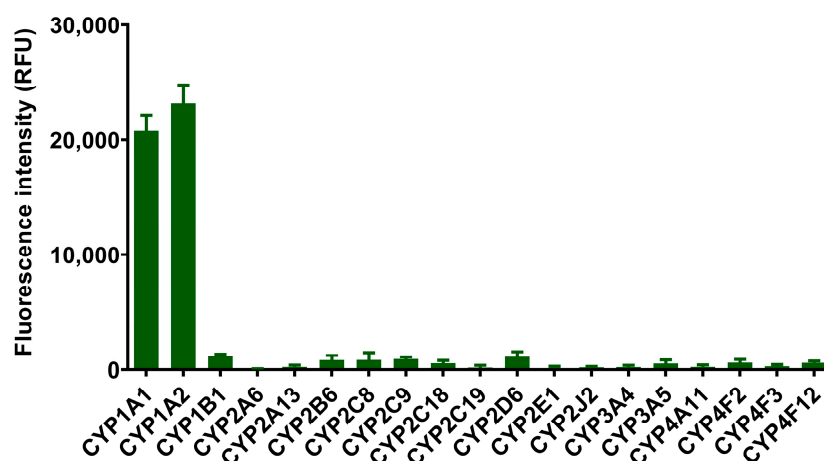


Figure 2. Fluorescence response of **ERNM** that incubated with different subtypes of human CYPs. Data are shown as the mean \pm SD.

2.4. Kinetic Behavior Analysis

The kinetic plot of CYP1A1/1A2 catalyzed **ERNM** O-demethylation was depicted to explore the interaction mode between CYP1A and **ERNM**. The CYP1A1 and CYP1A2 mediated demethylation of **ERNM** both followed kinetics of substrate inhibition (Supplementary Figure S5). The K_m values for demethylation catalyzed by CYP1A1 and CYP1A2 were determined as 1.0 ± 0.1 and 2.9 ± 0.5 μM , respectively (Table S1). The V_{max} values for demethylation catalyzed by CYP1A1 and CYP1A2 were determined as 1.92 ± 0.04 and 3.32 ± 0.15 nmol/min/nmol P450, respectively. These results implied a relatively high affinity and catalytic efficiency for the demethylated reaction of **ERNM**. Furthermore, the similar apparent kinetic parameters for CYP1A1- and CYP1A2-mediated demethylated reaction illustrate the highly consistent catalytic behaviors of CYP1A1 and CYP1A2 toward **ERNM**. The selectivity of **ERNM** and kinetic behavior of the CYP1A-mediated methylated reaction implied that the fluorescent probe **ERNM** enables the rapid and precise monitoring of the activity of CYP1A in complex bio-samples.

2.5. Colocalization Assay of ERNM toward ER

The systematic evaluation of **ERNM** confirmed its application in complex biosystems, subsequent work is related to the investigation of the subcellular localization of **ERNM** in living cells. Briefly, **ERNM** was co-incubated with a commercial ER-Tracker (red) in

A549 cells, and then imaged under two-photon (ERNM) and single-photon (ER-Tracker) excitation conditions using confocal fluorescence microscope. As shown in Figure 3, the green fluorescence signal produced by ERNM correlated well with the signal of commercial ER-Tracker. The overlapped fluorescence indicated that ERNM could image CYP1A in biosystems and exclusively target the ER.

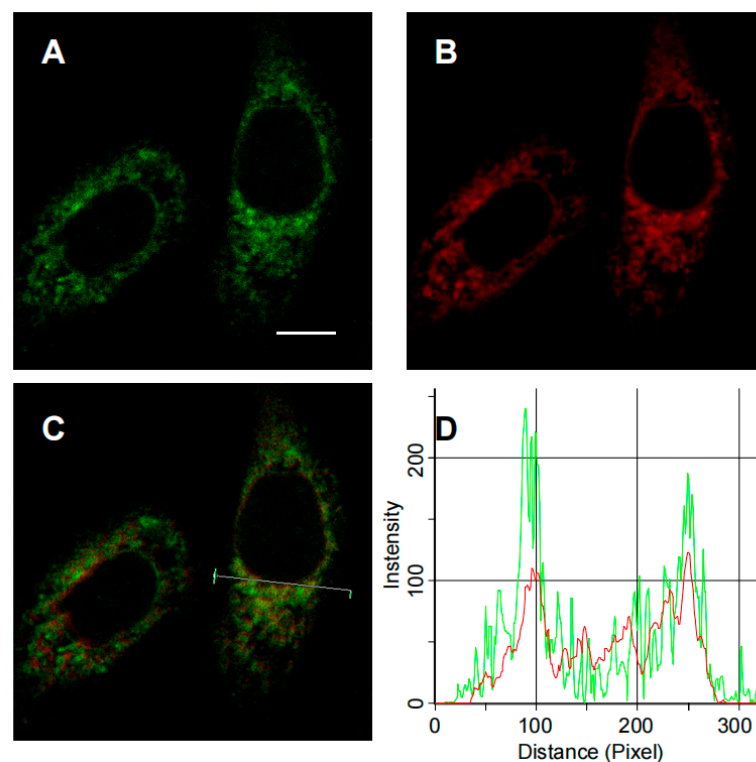


Figure 3. (A) Two-photon confocal fluorescence images of CYP1A in A549 treated with ERNM at the channel 520–560 nm; (B) ER-Tracker; (C) merge image; (D) fluorescence intensity for the region of interest (line in panel (C)), the green line represented the fluorescence intensity for ERNM and the red line represented the fluorescence intensity for ER-Tracker. Scale bar is 10 μm , as shown in panel A.

2.6. Bioimaging of CYP1A in Liver Slice

As mentioned above, CYP1A is an important metabolizing enzyme expressed in the liver that mediates the oxidative metabolism of many clinical drugs and environmental toxicants. Herein, we used ERNM to image CYP1A in rat liver slice by two-photon microscopy. After staining with ERNM, the two-photon excited fluorescence signal caused by CYP1A was detected in liver slice (Figure 4A). The multidimensional tissue images indicated the usability of ERNM for depth imaging CYP1A (Figure 4B). The obtained different depth of images showed the expression of CYP1A. Therefore, ERNM displayed good capability for deep tissue penetration, which facilitates the direct detection of CYP1A in tissue.

2.7. Bioimaging of CYP1A under ER Stress

Research continues to validate that the functionality level of CYP1A can be modulated under multiple pathological conditions, including nonalcoholic fatty liver disease, cancer, and type II diabetes, since CYP1A is an ER-locating protein that is associated with the production of oxidative stress [6,7]. For example, CYP1A was reported to cause an accumulation of reactive oxidative species and sometimes may work as a pro-oxidant agent in its expression region. Therefore, in the present study, the regulation of CYP1A under ER injury, which was induced by ER stress inducer dithiothreitol (DTT; Osowski and Urano, 2011), was investigated using the developed ER-targeting two-photon fluorescent probe ERNM.

As shown in Figure 5A,B, there were significant fluctuations in the CYP1A activity imaged by ERNM, and the graphical quantification of average fluorescence intensity indicated that the CYP1A activity reached the peak at 2 h in DTT-induced ER stress cell model. Meanwhile, the protein level of CYP1A followed the similar trend with the activity level of CYP1A detected by ERNM, implying that the changes in CYP1A activity were attributed to the regulation of protein expression of CYP1A in ER stress state. Notably, the variation trend of CHOP, a marker for the production of ER stress also increased at the beginning and then declined with time. The correlation between changes in activity and protein level of CYP1A and changes in the state of ER further confirmed the close association of ER state and ER-locating CYP1A. These results indicated that ERNM could image CYP1A in living cells, which is useful for evaluating the changes in CYP1A activity and protein level under ER stress and some ER-related diseases.

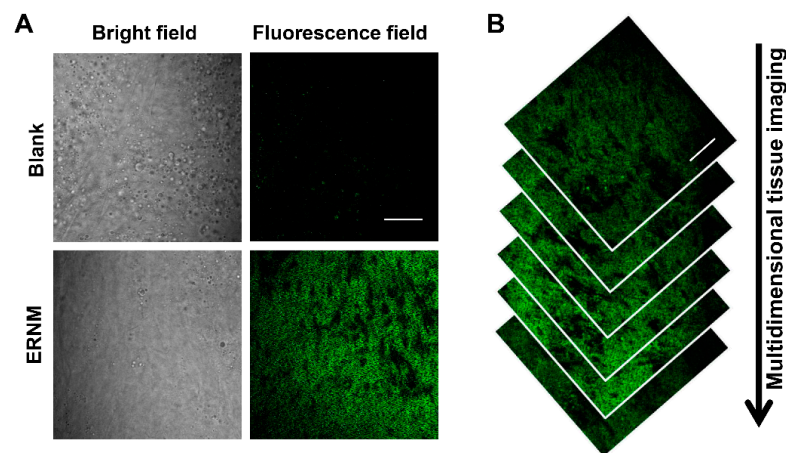


Figure 4. (A) Two-photon fluorescence images of the CYP1A in rat liver slices with ERNM. (B) Multidimensional two-photon fluorescence images of liver tissue treated with ERNM. Scale bar: 100 μ m.

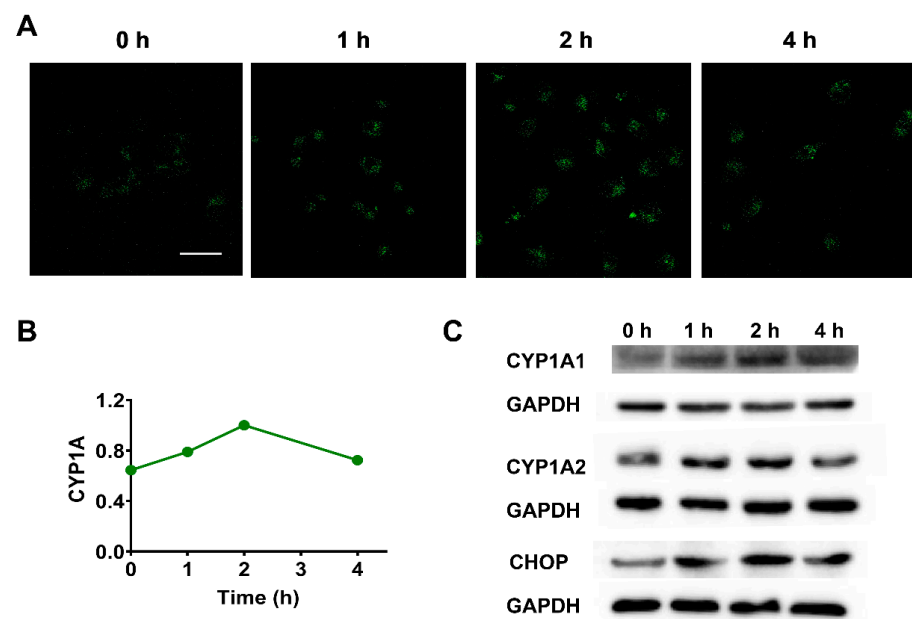


Figure 5. Two-photon fluorescence images of DTT pre-treated A549 cells. (A) Fluorescence images of DTT (2.5 mM, 0–4 h) pre-treated A549 cells that stain with ERNM. (B) Graphical quantification of average fluorescence intensity of images belonging to different experimental groups. (C) The protein level of CYP1A and CHOP in experimental groups treated with 2.5 mM DTT for different durations. Scale bar: 50 μ m.

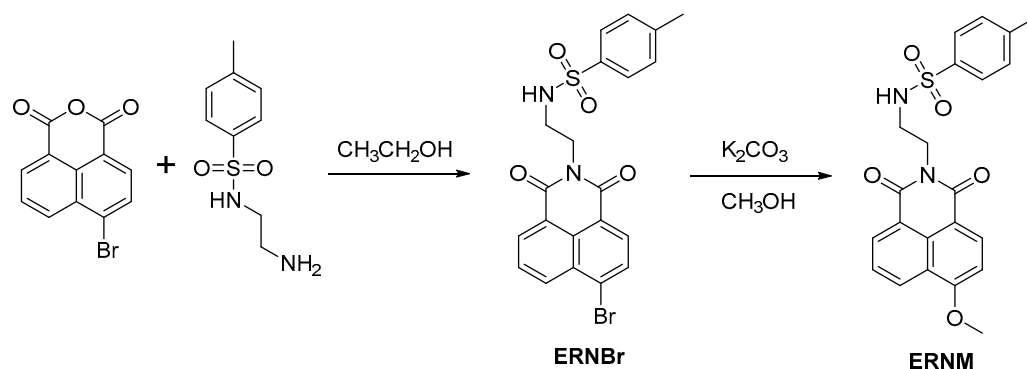
3. Materials and Methods

3.1. Instruments and Reagents

cDNA-expressed recombinant human CYP (rhCYP) isoforms including rhCYP1A1, rhCYP1A2, rhCYP1B1, rhCYP2A6, rhCYP2B6, rhCYP2C8, rhCYP2C9, rhCYP2C18, rhCYP2C19, rhCYP2D6, rhCYP2E1, rhCYP2J2, rhCYP3A4, rhCYP3A5, rhCYP4A11, rhCYP4F2, rhCYP4F3, and rhCYP4F12 were purchased from BD Biosciences (Woburn, MA, USA). Cofactors involved in the *in vitro* assay, such as β -nicotinamide adenine dinucleotide phosphate (NADP⁺), glucose-6-phosphate dehydrogenase, and glucose-6-phosphate were purchased from Sigma-Aldrich (St. Louis, MO, USA). The chemical inhibitors for different CYP subtypes including clomethiazole, sulfaphenazole, omeprazole, and quinidine were purchased from Sigma-Aldrich (St. Louis, MO, USA); ketoconazole and montelukast were obtained from Meilunbio (Dalian, China); N,N',N''-triethylene thiophosphoramidate (TEPA) was purchased from Aladdin (Shanghai, China). The mixed gender 150-donor pooled human liver microsomes were purchased from BIOIVT elevating science (Baltimore, MD, USA). ER-Tracker Red was purchased from Yeasen Biotechnology Co., Ltd. The solvents for liquid chromatography were obtained from Tedia (Fairfield, OH, USA). All other reagents were of the highest grade as commercially available.

¹H-NMR and ¹³C-NMR spectra were recorded using a Bruker spectrometer (in CDCl₃). High-resolution mass spectral (HR-MS) analyses were measured using an AB sciex X500R. Incubation samples were measured on a BioTek Synergy H1 Hybrid Multi-Mode Microplate Reader. The cells and tissue samples were imaged by a FV1000 MPF confocal laser scanning microscope (Olympus, Tokyo, Japan).

3.2. Synthesis of Probe



4-bromo-1,8-naphthalic anhydride (138.5 mg, 0.50 mmol) and *N*-tosylethylenediamine (117.8 mg, 0.55 mmol) were dissolved in 30 mL ethanol. The reaction mixture was refluxed for 16 h, the solvent was removed in vacuum, and the residual solid was purified by chromatography (silica gel, EtOAc–hexane as eluent, 1:4, *v/v*) to afford 160.5 mg **ERNBr**. ¹H NMR (600 MHz, CDCl₃) δ 8.62–8.54 (m, 2H), 8.32 (d, *J* = 7.8 Hz, 1H), 8.05 (d, *J* = 7.8 Hz, 1H), 7.86 (dd, *J* = 8.4, 7.4 Hz, 1H), 7.52 (d, *J* = 8.2 Hz, 2H), 6.73 (d, *J* = 8.0 Hz, 2H), 5.11 (t, *J* = 5.3 Hz, 1H), 4.29–4.25 (m, 2H), 3.49 (dd, *J* = 11.1, 5.5 Hz, 2H), 1.95 (s, 3H). ¹³C NMR (150 MHz, CDCl₃) δ 164.06, 163.99, 142.68, 137.17, 133.64, 132.28, 131.42, 131.16, 130.73, 130.58, 129.18, 128.96, 128.17, 126.67, 122.61, 121.71, 42.46, 39.23, 21.14. HRMS (ESI positive) calcd for [M + H]⁺ 473.0165, found 473.0176.

A mixture of **ERNBr** (118 mg, 0.25 mmol) and K₂CO₃ (347.5 g, 2.5 mmol) in 30 mL CH₃OH was refluxed for 10 h, the solvent was removed in vacuum, and the residual solid was purified by chromatography (silica gel, EtOAc–hexane as eluent, 1:4, *v/v*) to afford 80.5 mg **ERNM**. ¹H NMR (600 MHz, CDCl₃) δ 8.58 (d, *J* = 8.3 Hz, 1H), 8.50 (d, *J* = 7.2 Hz, 1H), 8.47 (d, *J* = 8.3 Hz, 1H), 7.71 (t, *J* = 7.8 Hz, 1H), 7.52 (d, *J* = 8.1 Hz, 2H), 7.05 (d, *J* = 8.3 Hz, 1H), 6.71 (d, *J* = 8.0 Hz, 2H), 5.26 (t, *J* = 4.8 Hz, 1H), 4.27–4.23 (m, 2H), 4.16 (s, 3H), 3.47 (dd, *J* = 10.8, 5.2 Hz, 2H), 1.92 (s, 3H). ¹³C NMR (150 MHz, CDCl₃) δ 164.92, 164.41, 161.15, 142.55, 137.01, 133.87, 131.80, 129.42, 129.14, 129.06, 126.68, 126.02, 123.44, 121.89, 114.56,

105.28, 56.36, 42.83, 38.93, 21.09. HRMS (ESI positive) calcd for $[M + H]^+$ m/z 425.1166, found m/z 425.1167.

3.3. The pH Effects on Fluorescence Signal of Probe Substrate ERNM and Probe Product ERNO

The effect of pH variation, within the range from 3 to 12, on the fluorescence intensity of probe substrate **ERNM** and the corresponding probe product **ERNO** was examined (the in-system concentration of **ERNM** and **ERNO** in the incubation system is 10 μ M). The intensity of fluorescence signal at 558 nm that was excited at 450 nm was recorded. Data were analyzed using GraphPad Prism 8.0 (GraphPad Software, Inc., San Diego, CA, USA).

3.4. The Influence of Analytes on the Fluorescence Response of ERNM

The effect of various analytes in reaction system including common ion (Mn^{2+} , Ca^{2+} , Mg^{2+} , Ni^{2+} , Zn^{2+} , Sn^{4+} , K^+ , Fe^{3+} , Na^+ , Ba^{2+}), amino acid (Ser, Trp, Gly, Arg, Cys), and GSH on the fluorescence response of **ERNM** was examined at the concentration of 10 μ M in the presence of NADPH-generating systems. The fluorescence signal of incubation samples in the presence of various analytes and recombinant human CYP1A1 and CYP1A2 were compared with samples in the absence of analytes. The total volume of the incubation mixture is 200 μ L.

3.5. In Vitro Assay for CYP Activity

The incubation sample consisted of NADPH-generating system (including $NADP^+$, magnesium chloride, glucose-6-phosphate, and glucose-6-phosphate dehydrogenase), and human liver microsomes or recombinant human CYP enzyme in potassium phosphate buffer (100 mM, pH 7.4). The total volume of the incubation mixture is 200 μ L. Fluorescent substrate was dissolved in DMSO, and was pre-diluted to the working concentrations. If necessary, blank samples without NADPH or without enzymes will be set up as negative controls. The incubation reaction was initiated by adding $NADP^+$ after pre-incubation at 37 °C for 3 min. In addition, ice acetonitrile (100 μ L) was added into the incubation samples for terminating the reaction progress.

3.6. Fluorescence Response of ERNM toward CYP1A and Various Human CYPs

To reveal the enzyme specificity for **ERNM**, the human recombinant CYP enzymes including CYP1A1, CYP1A2, CYP1B1, CYP2A6, CYP2A13, CYP2B6, CYP2C8, CYP2C9, CYP2C18, CYP2C19, CYP2D6, CYP2E1, CYP2J2, CYP3A4, CYP3A5, CYP4A11, CYP4F2, CYP4F3, and CYP4F12 (15 nM) were incubated with **ERNM** (the in-system concentration of **ERNM** in the incubation system is 10 μ M) in 200 μ L of the incubation mixture in the presence of NADPH-generating systems. After incubation for 30 min at 37 °C, the dealkylated metabolite was measured by quantifying the intensity of fluorescence signal at 558 nm that was excited at 450 nm. Data were analyzed using GraphPad Prism 8.0 (GraphPad Software, Inc., San Diego, CA, USA).

To confirm the linear range of **ERNM** in response to different enzyme concentrations of CYP1A1 and CYP1A2, the CYP1A1 (0.5, 1, 2.5, 5, 7.5, 10, 15, and 20 nM) and CYP1A2 (0.5, 1, 2.5, 5, 7.5, 10, 15, and 20 nM) were incubated with **ERNM** (the in-system concentration of **ERNM** in the incubation system is 10 μ M) in the presence of NADPH-generating systems, respectively. The total volume of the incubation mixture is 200 μ L. After incubation for 30 min, the formation of the dealkylated metabolite for **ERNM** was measured by quantifying the intensity of fluorescence signal at 558 nm that was excited at 450 nm. Data were analyzed using GraphPad Prism 8.0 (GraphPad Software, Inc., San Diego, CA, USA).

3.7. Inhibition Assay Using Selective Chemical Inhibitors for Different CYP Subtypes

The velocities of methylation of **ERNM** in HLM with the absence or presence of selective inhibitors for various CYP subtypes were measured to identify the major contribution of CYP1A toward the oxidative biotransformation of **ERNM**. In brief, **ERNM** (the in-system concentration of **ERNM** in the incubation system is 10 μ M) was incubated in HLM in the

absence (control samples) or presence (inhibitory samples) of selective chemical inhibitors for human different CYP subtypes in potassium phosphate buffer (100 mM, pH 7.4) with NADPH-generating system. The incubation mixture is 200 μ L. The involved chemical specific inhibitors and their work concentrations in the incubation system were listed as follows: α -Naphthoflavone (2.5 μ M), a selective chemical inhibitor for CYP1A subfamily that consists of CYP1A1 and CYP1A2 subtypes; N,N',N''-triethylene thiophosphoramidate (TEPA, 50 μ M), a selective chemical inhibitor for CYP2B6; omeprazole (20 μ M), a selective chemical inhibitor for CYP2C19; montelukast (2 μ M), a selective chemical inhibitor for CYP2C8; sulfaphenazolum (10 μ M), a selective chemical inhibitor for CYP2C9; quinidine (10 μ M), a selective chemical inhibitor for CYP2D6; clomethiazole (50 μ M), a selective chemical inhibitor for CYP2E1; ketoconazole (1 μ M), a selective chemical inhibitor for CYP3A subfamily that mainly consists of CYP3A4 and CYP3A5 subtypes. Inhibition by TEPA for CYP2B6 were examined by adding ERNM after pre-incubation with NADPH-generating system at 37 °C for 30 min. The intensity of fluorescence signal at 558 nm for samples treated with the absence or presence of selective inhibitors for various CYP subtypes was measured. In addition, the residual activity of samples was calculated by the percentage of fluorescence signal for the chemical inhibition group to the control group, with the absence of specific inhibitors. Data were analyzed using GraphPad Prism 8.0 (GraphPad Software, Inc., San Diego, CA, USA).

3.8. Enzyme Kinetic Analysis

Briefly, CYP1A1 (5 nM) or CYP1A2 (5 nM) were incubated with ERNM (1, 5, 10, 15, 50, 100, 200 μ M) in 200 μ L of the incubation mixture in the presence of NADPH-generating systems. After incubation for 30 min, the dealkylated metabolite was measured by quantifying the intensity of fluorescence signal at 558 nm that was excited at 450 nm. Data were analyzed using GraphPad Prism 8.0 (GraphPad Software, Inc., San Diego, CA, USA).

3.9. Cell Culture and Imaging

A549 cells were grown in RPMI-1640 culture medium (containing 10% FBS). A549 cells were seeded and incubated at 37 °C overnight. Then, A549 cells divided into different experimental groups were treated with DTT (dithiothreitol, the in-system concentration of DTT in the incubation system is 2.5 mM) for 0, 1, 2, and 4 h. The adherent cells were washed, and ERNM was added into the cell culture media (the in-system concentration of ERNM in the incubation system is 25 μ M) and incubated for 60 min. Then, the cells were rinsed with PBS for at least 3 times to remove the extracellular probe. The cell images were obtained using confocal microscope (Olympus, FV1000), and the excitation wavelength was set at 800 nm and fluorescent emission windows of 520–560 nm.

3.10. Preparation of Liver Slices and Imaging

Slices were prepared from the liver of 8-week-old male SD rat. The liver was cut into squares of appropriate size, and an appropriate amount of OCT embedding agent was added for immersion in the tissue. Then, the tissue was frozen by nitrogen for 10–20 s. Thereafter, the tissue ice cubes were removed and immediately placed in the constant cold box microtome for the frozen section. The liver tissues were cut into 100 μ m in thickness. The liver slices were incubated with ERNM or only incubated with PBS (the in-system concentration of ERNM in the incubation system for liver slices is 25 μ M) at 37 °C for 60 min. Then, the slices were rinsed with PBS for at least 3 times to remove the extracellular probe. Images for liver tissues were obtained using confocal microscope (Olympus, FV1000), and excitation wavelength was set at 800 nm and fluorescent emission windows of 520–560 nm.

4. Conclusions

In summary, we developed a selective two-photon fluorescent molecular tool ERNM for the visualization of ER-targeting CYP1A. ERNM could target the ER and monitor the

fluctuation of CYP1A activity in living cells and tissues. The detection ability of ERNM for the functionality level of CYP1A under ER stress was further confirmed. Based on the ER-targeting two-photon probe for CYP1A, the close association of ER state and ER-locating CYP1A was confirmed, which would promote the understanding of CYP1A biofunctions in ER-related diseases.

Supplementary Materials: The following supporting information can be downloaded at: <https://www.mdpi.com/article/10.3390/molecules28083472/s1>, Table S1. Kinetic parameters of ERNM O-demethylation determined in CYP1A1 and CYP1A2; Figure S1. Fluorescence spectra and fluorescence intensity of ERNM that incubated with 7.5 nM CYP1A1 and 7.5 nM CYP1A2 with the prolonging of time; Figure S2. The effects of pH values on the fluorescence intensity of ERNM and its metabolite ERNH (2.5 μ M); Figure S3. Inhibitory effects of selective CYP inhibitors on ERNM O-demethylation in human liver microsomes; Figure S4. Fluorescence responses of ERNM towards CYP1A1 and CYP1A2 in the presence of various analytes; Figure S5. Kinetic plots of ERNM O-demethylation in CYP1A1 and CYP1A2; Figure S6. ^1H NMR of ERNB r ; Figure S7. ^{13}C NMR of ERNB r ; Figure S8. ^1H NMR of ERNM; Figure S9. ^{13}C NMR of ERNM; Figure S10. HRMS spectrum of ERNM.

Author Contributions: Conceptualization, J.N. and L.F.; methodology, C.S. and Y.W.; validation, X.T. and Y.A.; investigation, C.S. and Y.W.; writing—original draft preparation, J.N. and L.F.; writing—review and editing, J.N., X.X., X.L., X.M. and L.F.; project administration, J.N., L.D. and L.F. All authors have read and agreed to the published version of the manuscript.

Funding: The authors thank the National Natural Science Foundation of China (82174228 and 82004211), Research on National Reference Material and Product Development of Natural Products (SG030801, Beijing Polytechnic), open Research Fund of the School of Chemistry and Chemical Engineering, Henan Normal University for support (2021YB07, China), and Key Laboratory of Emergency and Trauma (Hainan Medical University), Ministry of Education (Grant. KLET-202111) for financial support.

Institutional Review Board Statement: The animal study protocol was approved by the Ethics Committee of Dalian Medical University (AEE19047, September 2019).

Informed Consent Statement: Not applicable.

Data Availability Statement: Not applicable.

Conflicts of Interest: The authors declare that the research was conducted in the absence of any commercial or financial relationships that could be construed as a potential conflict of interest.

Sample Availability: Samples of ERNM and ERNH are available from the authors.

References

1. Wei, P.; Zhang, J.; Egan-Hafley, M.; Liang, S.; Moore, D.D. The nuclear receptor CAR mediates specific xenobiotic induction of drug metabolism. *Nature* **2000**, *407*, 920–923. [[CrossRef](#)] [[PubMed](#)]
2. Guengerich, F.P. Roles of cytochrome P450 enzymes in pharmacology and toxicology: Past, present, and future. *Adv. Pharmacol.* **2022**, *95*, 1–47. [[CrossRef](#)] [[PubMed](#)]
3. Yuan, J.; Lu, W.Q.; Zou, Y.L.; Wei, W.; Zhang, C.; Xie, H.; Chen, X.M. Influence of aroclor 1254 on benzo(a)pyrene-induced DNA breakage, oxidative DNA damage, and cytochrome P4501A activity in human hepatoma cell line. *Environ. Toxicol.* **2009**, *24*, 327–333. [[CrossRef](#)] [[PubMed](#)]
4. Klomp, F.; Wenzel, C.; Drozdziak, M.; Oswald, S. Drug-Drug Interactions Involving Intestinal and Hepatic CYP1A Enzymes. *Pharmaceutics* **2020**, *12*, 1201. [[CrossRef](#)] [[PubMed](#)]
5. Lu, J.; Shang, X.; Zhong, W.; Xu, Y.; Shi, R.; Wang, X. New insights of CYP1A in endogenous metabolism: A focus on single nucleotide polymorphisms and diseases. *Acta Pharm. Sin. B* **2020**, *10*, 91–104. [[CrossRef](#)]
6. Melchini, A.; Catania, S.; Stancanelli, R.; Tommasini, S.; Costa, C. Interaction of a functionalized complex of the flavonoid hesperetin with the AhR pathway and CYP1A1 expression: Involvement in its protective effects against benzo(a)pyrene-induced oxidative stress in human skin. *Cell Biol. Toxicol.* **2011**, *27*, 371–379. [[CrossRef](#)]
7. Furue, M.; Uchi, H.; Mitoma, C.; Hashimoto-Hachiya, A.; Chiba, T.; Ito, T.; Nakahara, T.; Tsuji, G. Antioxidants for Healthy Skin: The Emerging Role of Aryl Hydrocarbon Receptors and Nuclear Factor-Erythroid 2-Related Factor-2. *Nutrients* **2017**, *9*, 223. [[CrossRef](#)]
8. Hotamisligil, G.S. Endoplasmic reticulum stress and the inflammatory basis of metabolic disease. *Cell* **2010**, *140*, 900–917. [[CrossRef](#)]

9. Lemmer, I.L.; Willemsen, N.; Hilal, N.; Bartelt, A. A guide to understanding endoplasmic reticulum stress in metabolic disorders. *Mol. Metab.* **2021**, *47*, 101169. [[CrossRef](#)]
10. Puntarulo, S.; Cederbaum, A.I. Production of reactive oxygen species by microsomes enriched in specific human cytochrome P450 enzymes. *Free Radic. Biol. Med.* **1998**, *24*, 1324–1330. [[CrossRef](#)]
11. Al-Dhfyhan, A.; Alhoshani, A.; Korashy, H.M. Aryl hydrocarbon receptor/cytochrome P450 1A1 pathway mediates breast cancer stem cells expansion through PTEN inhibition and beta-catenin and Akt activation. *Mol. Cancer* **2017**, *16*, 14. [[CrossRef](#)] [[PubMed](#)]
12. Liu, H.W.; Chen, L.; Xu, C.; Li, Z.; Zhang, H.; Zhang, X.B.; Tan, W. Recent progresses in small-molecule enzymatic fluorescent probes for cancer imaging. *Chem. Soc. Rev.* **2018**, *47*, 7140–7180. [[CrossRef](#)]
13. Zhang, J.J.; Chai, X.Z.; He, X.P.; Kim, H.J.; Yoon, J.Y.; Tian, H. Fluorogenic probes for disease-relevant enzymes. *Chem. Soc. Rev.* **2019**, *48*, 683–722. [[CrossRef](#)] [[PubMed](#)]
14. Ning, J.; Liu, T.; Dong, P.; Wang, W.; Ge, G.; Wang, B.; Yu, Z.; Shi, L.; Tian, X.; Huo, X.; et al. Molecular Design Strategy to Construct the Near-Infrared Fluorescent Probe for Selectively Sensing Human Cytochrome P450 2J2. *J. Am. Chem. Soc.* **2019**, *141*, 1126–1134. [[CrossRef](#)]
15. Feng, L.; Tian, X.; Yao, D.; Yu, Z.; Huo, X.; Tian, Z.; Ning, J.; Cui, J.; James, T.D.; Ma, X. A practical strategy to develop isoform-selective near-infrared fluorescent probes for human cytochrome P450 enzymes. *Acta Pharma. Sinica B* **2021**, *12*, 1976–1986. [[CrossRef](#)]
16. Feng, L.; Ning, J.; Tian, X.; Wang, C.; Yu, Z.; Huo, X.; Xie, T.; Zhang, B.; James, T.D.; Ma, X. Fluorescent probes for the detection and imaging of Cytochrome P450. *Coord. Chem. Rev.* **2021**, *437*, 213740. [[CrossRef](#)]
17. Yan, F.; Cui, J.; Wang, C.; Tian, X.; Li, D.; Wang, Y.; Zhang, B.; Feng, L.; Huang, S.; Ma, X. Real-time quantification for sulfite using a turn-on NIR fluorescent probe equipped with a portable fluorescence detector. *Chin. Chem. Lett.* **2022**, *33*, 4219–4222. [[CrossRef](#)]
18. Ning, J.; Wang, W.; Ge, G.; Chu, P.; Long, F.; Yang, Y.; Peng, Y.; Feng, L.; Ma, X.; James, T.D. Targeted Enzyme Activated Two-Photon Fluorescent Probes: A Case Study of CYP3A4 Using a Two-Dimensional Design Strategy. *Angew Chem. Int. Ed.* **2019**, *58*, 9959–9963. [[CrossRef](#)]
19. Lu, Q.; Wu, C.J.; Liu, Z.Q.; Niu, G.L.; Yu, X.Q. Fluorescent AIE-Active Materials for Two-Photon Bioimaging Applications. *Front. Chem.* **2020**, *8*, 617463. [[CrossRef](#)]
20. Noh, C.K.; Lim, C.S.; Lee, G.H.; Cho, M.K.; Lee, H.W.; Roh, J.; Kim, Y.B.; Lee, E.; Park, B.; Kim, H.M.; et al. A Diagnostic Method for Gastric Cancer Using Two-Photon Microscopy with Enzyme-Selective Fluorescent Probes: A Pilot Study. *Front. Oncol.* **2021**, *11*, 634219. [[CrossRef](#)]
21. Ning, J.; Tian, Z.; Wang, J.; Wang, B.; Tian, X.; Yu, Z.; Huo, X.; Feng, L.; Cui, J.; James, T.D.; et al. Rational Design of a Two-Photon Fluorescent Probe for Human Cytochrome P450 3A and the Visualization of Mechanism-Based Inactivation. *Angew Chem. Int. Ed.* **2022**, *61*, e202113191. [[CrossRef](#)] [[PubMed](#)]
22. Dai, Z.R.; Ge, G.B.; Feng, L.; Ning, J.; Hu, L.H.; Jin, Q.; Wang, D.D.; Lv, X.; Dou, T.Y.; Cui, J.N.; et al. A Highly Selective Ratiometric Two-Photon Fluorescent Probe for Human Cytochrome P450 1A. *J. Am. Chem. Soc.* **2015**, *137*, 14488–14495. [[CrossRef](#)] [[PubMed](#)]
23. Dai, Z.R.; Feng, L.; Jin, Q.; Cheng, H.; Li, Y.; Ning, J.; Yu, Y.; Ge, G.B.; Cui, J.N.; Yang, L. A practical strategy to design and develop an isoform-specific fluorescent probe for a target enzyme: CYP1A1 as a case study. *Chem. Sci.* **2017**, *8*, 2795–2803. [[CrossRef](#)] [[PubMed](#)]
24. Zhang, X.; Zhou, Y.; Gu, X.; Cheng, Y.; Hong, M.; Yan, L.; Ma, F.; Qi, Z. Synthesis of a selective ratiometric fluorescent probe based on Naphthalimide and its application in human cytochrome P450 1A. *Talanta* **2018**, *186*, 413–420. [[CrossRef](#)] [[PubMed](#)]

Disclaimer/Publisher’s Note: The statements, opinions and data contained in all publications are solely those of the individual author(s) and contributor(s) and not of MDPI and/or the editor(s). MDPI and/or the editor(s) disclaim responsibility for any injury to people or property resulting from any ideas, methods, instructions or products referred to in the content.